Materials and Design 30 (2009) 1581–1587

Contents lists available at ScienceDirect

Materials and Design

journal homepage: www.elsevier.com/locate/matdes

Evaluation of AISI 316L stainless steel welded plates in heavy petroleum environment

Cleiton Carvalho Silva [a], Jesualdo Pereira Farias [a], Hosiberto Batista de Sant'Ana [b,*]

[a] Department of Materials and Metallurgical Engineering, Federal University of Ceará, Brazil
[b] Department of Chemical Engineering, Federal University of Ceará, Fortaleza, 60455-760 Ceara, Brazil

ARTICLE INFO

Article history:
Received 15 March 2007
Accepted 21 July 2008
Available online 6 August 2008

Keywords:
Ferrous metals and alloys (A)
Welding (D)
Corrosion (E)
Microstructure (F)

ABSTRACT

This work presents the study done on the effect of welding heating cycle on AISI 316L austenitic stainless steel corrosion resistance in a medium containing Brazilian heavy petroleum. AISI 316L stainless steel plates were welded using three levels of welding heat input. Thermal treatments were carried out at two levels of temperatures (200 and 300 °C). The period of treatment in all the trials was 30 h. Scanning electronic microscopy (SEM) and analysis of X-rays dispersive energy (EDX) were used to characterize the samples. Weight loss was evaluated to determine the corrosion rate. The results show that welding heating cycle is sufficient to cause susceptibility to corrosion caused by heavy petroleum to the heat affected zone (HAZ) of the AISI 316L austenitic stainless steel.

1. Introduction

Due to severe working conditions, such as high temperatures and contact with fluids of high level of corrosiveness, the equipments in the units of petroleum refinery may suffer various types of problems associated with corrosion, due to the presence of naphthenic acids [1–4], oxygen and carbonic acid [2,5], hydrogen sulfide [6], solid petroleum adhered [7], stress corrosion cracking [8] and others. For this reason, the equipment used in the petroleum and gas processing industries is made with a material that combines both good mechanical properties and excellent resistance to corrosion [9]. The stainless steel stands out among the types of materials that have both these characteristics for the fact that they can be fully applied in the manufacturing of equipment or can be used as coating. The second option is, in many cases, the most attractive from economical point of view [10]. Besides being resistant to corrosion, the stainless steel must have other qualities such as good weldability, since welding is largely done in the manufacturing and repairing of the equipment in the petroleum industry. Especially, AISI 316L austenitic stainless steel has been popularly used as lining in the repair of petroleum distillation column in refineries which process naphthenic crudes, despite its chemical composition, mainly molybdenum contents (2% approximately), that confer to steel a superior resistance to naphthenic acid [1,8,10].

The stainless steel is likely to have various metallurgical problems when exposed to certain temperature ranges. During the welding process, the thermal cycle is capable of submitting the heat affected zone (HAZ) of this material to these critical temperature ranges, which are responsible for the formation of intermetallic phases such as sigma (σ), chi (χ) and Laves, and unwanted precipitates ($M_{23}C_6$) [9,11,12]. Very often the adequate choice of the type of steel and of the welding parameters may result in an increase in the lifetime of the equipment. While studying the effect of the welding heat cycle on the resistance to corrosion of a ferritic stainless steel HAZ in a medium containing petroleum, Silva et al. [13] noticed that corrosion occurred preferentially in the HAZ region, and that the increase in the welding heat input contributes to the increase in corrosion, making the influence of welding on the corrosion resistance of the material clear.

For the fact that it has good resistance to corrosion, the AISI 316L austenitic stainless steel has been currently used in the petroleum and natural gas industries for the internal coating (lining) of petroleum distillation columns. However, the information about the response of this type of steel in a medium containing heavy petroleum and about the effects caused by welding on the resistance to corrosion is rather scarce.

The objective of this work is to contribute to the study of the AISI 316 austenitic stainless steel corrosion resistance used in Brazilian petroleum refinery environment, including the aspects related to the effect of the welding parameters (heat input) on microstructure and corrosion resistance of the heat affected zone, besides providing information to the industrial sector concerning the use of this material, with the aim to improve the reliability and the equipment lifetime, as well as to allow for cost reduction.

* Corresponding author. Tel.: +55 85 3366 9611; fax: +55 85 3366 9610.
E-mail address: hbs@ufc.br (H.B. de Sant'Ana).

0261-3069/$ - see front matter © 2008 Elsevier Ltd. All rights reserved.
doi:10.1016/j.matdes.2008.07.050

2. Experimental

AISI 316L austenitic stainless steel was used as base metal, whose chemical composition is shown in Table 1. The filler metal used was the AWS E 309MoL-16 austenitic stainless steel covered electrode with 2.5 mm diameter. The chemical composition of the filler metal, according to the manufacturer, is shown in Table 2.

Brazilian heavy petroleum (from Campos Basin), kindly supplied by *Centro de Pesquisas e Desenvolvimento Leopoldo Américo M. de Mello* – CENPES/PETROBRAS, was used in this work without any previous processing. Density, oil viscosity, and sulfur content were determined for the crude oil used in this work. The results of these analyses are shown in Table 3.

The bead on plate welding in the flat position was carried out on the AISI 316L austenitic stainless steel, with 50.0×150.0 mm dimensions and 3.0 mm thickness, with shielded metal arc welding process (SMAW). The procedure was carried out manually, with control of the welding speed. The multiprocess INVERSAL 450 welding source and a data acquisition system were used. Three levels of welding heat input were used in this work, by using a low arc energy in order to reduce the precipitation rate. The welding parameters used are shown in Table 4.

After the welding, the plates suffered a cleaning process to remove the slag. The plates were cut for the extraction of $12.0 \times 25.0 \times 3.0$ mm samples that contained a small proportion of the weld metal, the HAZ region and the base metal. One sample from each condition was submitted to thermal treatments when immersed in heavy crude oil in two different temperatures: 200 and 300 °C. This trial lasted for 30 h, by the samples immersed in heavy petroleum. It is important to notice that these test conditions are less harmful than those in the distillation towers where, besides the effect of temperature and type of petroleum, tension and fluid drainage can also be verified, which, among other factors, affect the process of corrosion in the material used for coating the tower.

Table 1
Chemical composition of the AISI 316L austenitic stainless steel (weight%)

C	Mn	Cr	P	S	Mo	Si	Ni	N
0.022	1.36	16.93	0.03	0.003	2.09	0.47	10.11	411[a]

[a] Value in ppm.

Table 2
Chemical composition of the AWS E309MoL-16 austenitic stainless steel weld metal (weight%)

C	Cr	Ni	Mo
0.03	23	13	2.5

Table 3
Petroleum characterization

Density (20/40)	API°	Viscosity 50 °C (mm^2/s)	Sulfur content (%m/m)
0.91042	16.8	240	0.56

Table 4
Welding parameters in DC$^+$

Current (A)	Tension (V)	Welding speed (cm/min)	Welding heat input (kJ/cm)
80	25	20.0	6.0
80	25	12.5	9.6
80	26	10.0	12.4

After the treatment, the samples were cleaned in kerosene for future evaluation of the surface. Scanning electronic microscopy (SEM) and energy of dispersive X-rays analysis (EDX) techniques were used to identify the type of corrosion products present and the influence of heavy oil in the samples. The samples were kept in a closed container, immersed in kerosene, until they were characterized in the SEM. This measure was taken in order to avoid a prolonged contact with air, which could cause atmospheric corrosion and consequent disguise of the results.

In order to determine the speed of the corrosive process of the material and the aggressiveness of the corrosive medium, the mass of the test objects was measured before and after the treatment in heavy petroleum to evaluate the loss of mass due to corrosion. The test objects were submitted to a chemical peeling with an alcoholic solution of 10% of nitric acid for approximately 20 min. A sample of each material as welded (with no treatment in petroleum) was immersed in the acid together with the treated samples to verify if loss of mass occurs due to the peeling. But no significant loss of mass was verified in the samples as welded.

The corrosion rate determination was calculated through Eq. (1), according to ASTM G1 standard [14].

$$\text{Corrosion rate} = K \times W/A \times t \times \rho \quad (1)$$

where K *is the* constant (mm h/year cm) -8.76×10^4, W *the* mass loss in grams, S *the* coupon exposed area in cm^2, t the time of exposure in hours and ρ is the specific mass of the steel (g/cm^3).

Metallographic samples were conventionally prepared by grinding with silicon carbides sandpaper and by diamond polishing. Electrolytic etching with 10% oxalic acid solution was done to reveal chromium carbides and austenite grain boundary. The microstructure was analyzed by optical microscope and scanning electron microscope (SEM).

3. Results and discussion

3.1. Microstructural characterization

The microstructure of the HAZ in the AISI 316L austenitic stainless steel for the three welding conditions is shown in Fig. 1a–c. It is possible to observe in these figures a narrow band in which the presence of δ-ferrite can be noticed among the grains of austenite, which form a microstructure with a similar aspect to that of the vermicular morphology of austenitic stainless weld metals. This happens because in this region the temperatures are enough to reach the austenite/δ-ferrite field. It can be also noticed that the extension of this band increases with the increase of the welding heat input.

The presence of δ-ferrite on HAZ can cause a partitioning of the chromium and nickel between ferrite and austenite. Cui and Lundin [15] evaluated the initial pitting corrosion into 316L austenitic stainless steel weld metal. These authors found that the initial corrosion attack occurred in austenite. This behavior was attributed to the increased micro-segregation of the cellular dendritic microstructure in the weld metal that results in the formation of chromium depleted in the cell cores. In this work, it was observed that the HAZ region formed by austenite/δ-ferrite was attacked by the acid products present in the petroleum. This is probably due to the partitioning of chromium and nickel as observed by Cui and Lundin [15].

In the farther region of the HAZ, other microstructural alterations were noticed, in the presence of spherical particles precipitates in the grain boundaries and matrix. Fig. 1d shows the microstructure of this region. The area in which the precipitates were observed is exactly the HAZ portion that reached 550–850 °C temperature, which constitutes the temperature range of

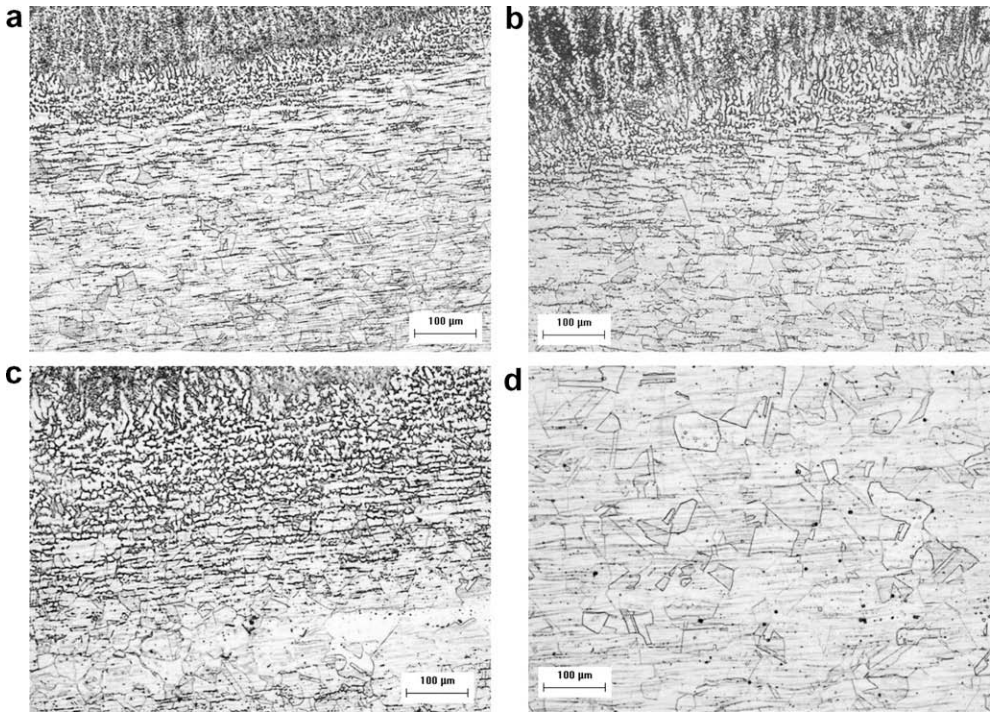

Fig. 1. HAZ microstructure of the AISI 316L steel welded with: (a) 6 kJ/cm, (b) 9 kJ/cm, (c) 12 kJ/cm and (d) enlarged HAZ to show some carbides precipitation (dark points). Etching: oxalic acid (200×).

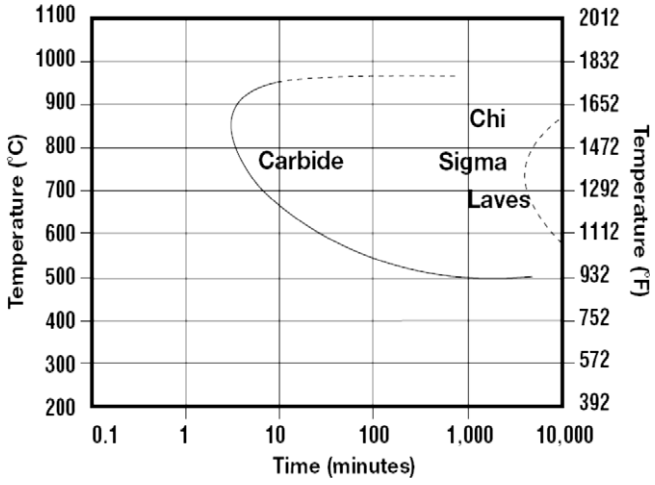

Fig. 2. Isothermal precipitation diagram for 316L stainless steel [12].

chromium carbides precipitation in austenitic stainless steels, as shown in Fig. 2. A preliminary analysis was made and it was verified that such particles were chromium carbides of the $M_{23}C_6$ type.

The presence of chromium carbides is quite harmful to the austenitic stainless steels corrosion resistance, turning them susceptible to the intergranular corrosion (IGC) [16,17]. The mechanism for which the intergranular corrosion happens in these steels is due to the sensitization phenomenon that consists in the chromium depletion zones adjacent to the rich-chromium precipitates, for example, $M_{23}C_6$ carbides [18]. Matula et al. [16] studied the intergranular corrosion of AISI 316L steel, and verified that the sensitization was the main microstructural alteration responsible for the susceptibility to corrosion of the steel.

It is well known that austenitic stainless steels can have their sensitization resistance increased by alterations in the chemical composition. Beneke and Sandenbergh [19] verified that the molybdenum addition in austenitic stainless steels containing nitrogen increases their resistance to the sensitization for delaying the chromium carbides precipitation and for increasing the passivation characteristics of steel. They also verified that the addition of nitrogen to the austenitic stainless steels containing molybdenum increases significantly the sensitization resistance for nitrogen concentrations above 0.125%. In spite of AISI 316L stainless steel containing 2–3% of Mo and some N content, chromium carbides precipitation in the welding conditions tested was observed by Luz et al. [20].

The sensitization evaluation and the susceptibility of intergranular corrosion can be evaluated by destructive test as ASTM A262. However, this method is limited to qualitative analysis. The double loop electrochemical potentiokinetic reactivation (DLEPR) test provides the sensitization degree of stainless steel by measuring the amount of chromium-depleted areas which are adjacent to the precipitates rich in chromium [16,17,21]. This method is a quanti-

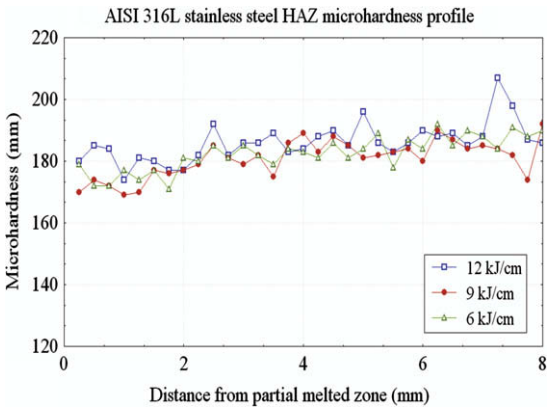

Fig. 3. HAZ microhardness profile of the sample welded with 12 kJ/cm.

tative evaluation and can be used to detect a degree of sensitization, even in materials that apparently have no presence of carbides precipitation in metallographic analysis. Luz et al. [20] used DLEPR test to identify the sensitized zone extension in type 316L austenitic stainless steels in similar conditions of this work, to verify the influence of welding on the sensitized zone extension and to report that this was of 1.3 mm for 9 kJ/cm welding heat input, and for 12 kJ/cm welding heat input, the length of sensitized zone was 2.6 mm. They also concluded that the DLEPR test was capable of detecting the sensitization in conditions in which the ASTM A262 [22] test can not detect.

The microhardness profiles of the HAZ for the three different energies used in this work are shown in Fig. 3. It is important to notice that even though the presence of chromium carbides precipitated in the HAZ of all welding conditions, has been verified , no significant hardness variations were observed in the 8 mm analyzed.

3.2. Surface characterization

The sample treated at 200 °C presented a layer of corrosion product on the surface, which almost completely covered the region adjoining the weld bead, as shown in Fig. 4a. In the zoom area (Fig. 4b), it is possible to observe the layer formation and the morphology of the corrosion product. The chemical analysis

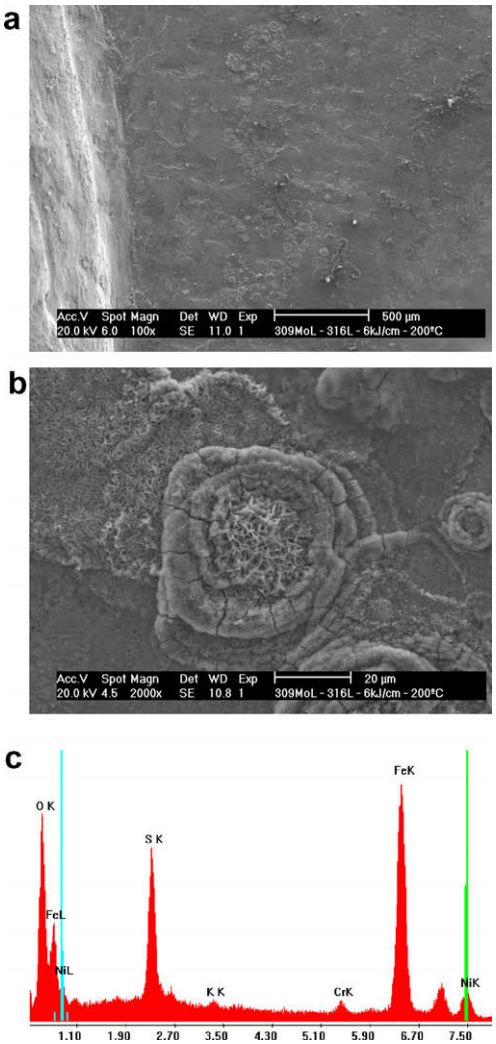

Fig. 4. (a) Region adjoining the weld bead, (b) corrosion products morphology and (c) chemical composition of the corrosion products by EDX analyses.

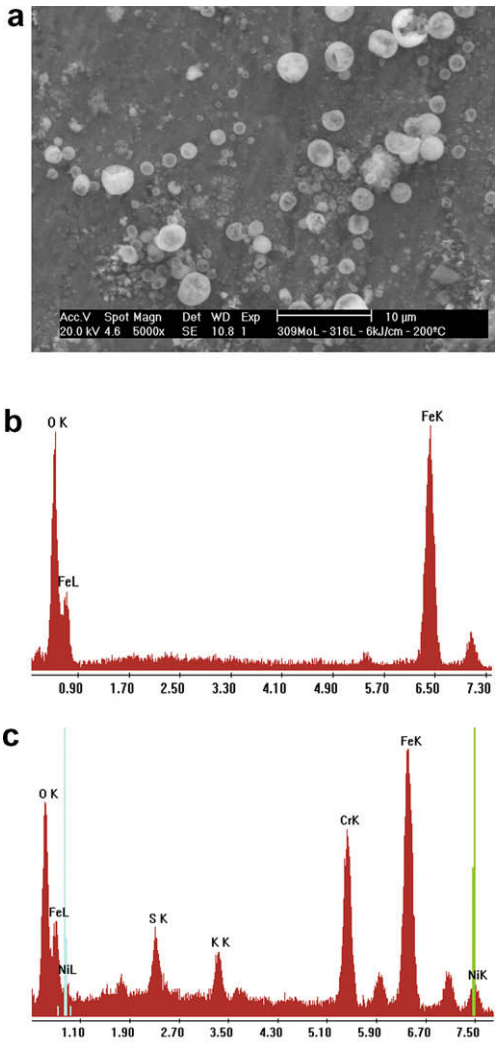

Fig. 5. (a) HAZ region far from the weld bead, (b) particles chemical composition by EDX and (c) layer chemical composition by EDX.

of the particles is shown in Fig. 4c and it indicates the presence of a high percentage of iron, oxygen and sulfur, suggesting that the layer is formed by iron oxide and sulphide. Cracks can also be observed in the formation of the tubercle morphology (Fig. 4b), which continuously exposes the substrate to the corrosive medium.

The HAZ region which is far from the weld bead is shown in Fig. 5a. Here a layer of corrosion product and a new nucleation on the layer can be observed. The chemical analysis of the particle and the layer is shown in Fig. 5b and c, respectively.

It has been noticed that the particles are iron oxide with a globular morphology. These particles in the shape of globules are similar to the ones found by Silva et al. [23] in their work, in which they evaluated the superficial corrosion caused by heavy petroleum from the Fazenda Alegre field in the state of Espírito Santo/Brazil. The layer presented a more complex chemical composition, in which, besides oxygen and iron, a large quantity of chrome and the presence of sulfur, nickel and potassium have been noticed. The presence of nickel and chrome is ascribed to the chemical composition of the steel. The sulfur may be associated to the oxide in the form of iron sulphide, and the potassium may be derived from the mineral salts present in heavy petroleum.

The formation of a layer with corrosion product was not noticed in the region of the base metal. However, a structure with a

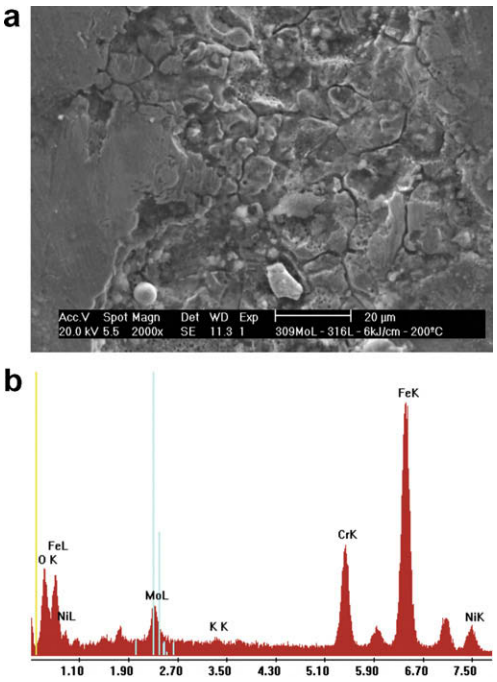

Fig. 6. (a) AISI 316L steel base metal, austenite grain boundary in detail and (b) chemical composition by EDX of the region indicated.

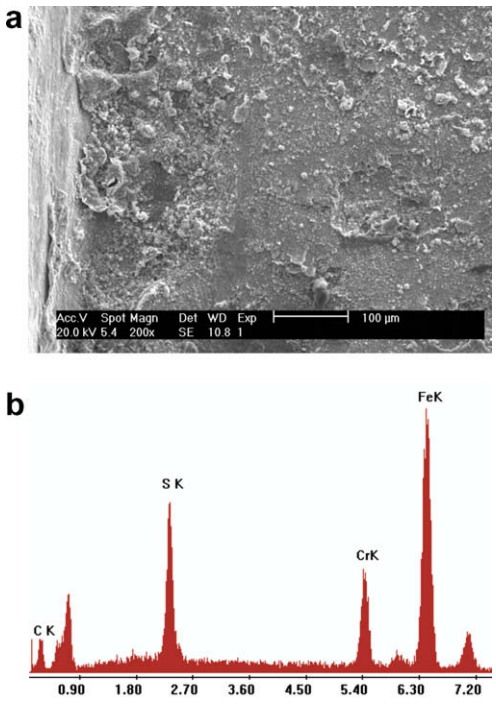

Fig. 7. (a) HAZ region adjoining the weld bead of the sample welded with 12 kJ/cm and treated at 300 °C, and (b) chemical analyses by EDX of the corrosion products shown in Fig. 6a.

'cracked' aspect similar to the contours of grains, in some cavities derived from the roughness of the material has been noticed. The amplified detail of one of these cavities is shown in Fig. 6a. The EDX analysis presented in Fig. 6b shows a small quantity of oxygen and the main components of the steel alloy, implying that the cracks are actually the austenite grain boundary that suffered the attack of the corrosive medium. While evaluating the action of corrosion in petroleum of the AISI 304 austenitic stainless steel, Machado et al. [24] noticed that the corrosion of the material, when it was submitted to heating ranging from room temperature to 200 and 300 °C, occurred mainly in the austenite grains boundary.

The presence of iron oxides and iron sulfides as corrosion products in the samples treated at 200 °C can be an indication of the action of corrosive substances containing oxygen and sulfur. In this temperature, some corrosion type's characteristics in petroleum refining units can act simultaneously, as the CO_2 and H_2S corrosion.

Carbonic acid encountered in petroleum can be formed by the presence of carbon dioxide (CO_2) dissolved in water, according

$$CO_2 + H_2O \rightarrow H_2CO_3 \quad (2)$$

This acid in contact with the steel surface reacts with the iron originating a corrosion process. Above 80 °C the predominant reaction is described by Eq. (3), where the product of the corrosion is the siderite ($FeCO_3$). However, for temperatures above 250 °C the magnetite formation (Fe_3O_4) is probable.

$$Fe + H_2CO_3 \rightarrow FeCO_3 + 2H^+ + 2e \quad (3)$$

Although only the effect of the presence of CO_2 is being considered separately, other substances can act affecting the corrosion rate together. Chernov [2], studying the carbonic acid corrosion, verified that the presence of H_2S in the mixture in a temperature range from 20 to 80 °C increases the corrosion rate from 1.5 to 2 times. Already for larger concentrations of H_2S and for temperatures between 100 and 250 °C, the corrosion process is decelerated by competition between H_2S and H_2CO_3. The presence of H_2S in oil is pointed as the main source to form iron sulfide as corrosion products.

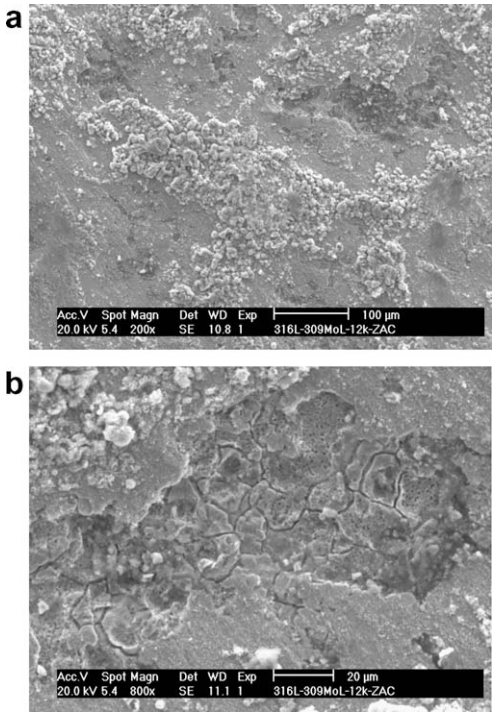

Fig. 8. (a) HAZ region far from the weld bead of the sample welded with 12 kJ/cm and treated at 300 °C and (b) austenite grain boundary in detail.

Generally speaking, the aspects of the surface of the samples welded with 6, 9 and 12 kJ/cm and treated at 300 °C were similar to those shown in Fig. 7a. A relatively consolidated layer of corrosion product has been noticed. The chemical analysis by EDX presented in Fig. 7b shows that the elements present are basically

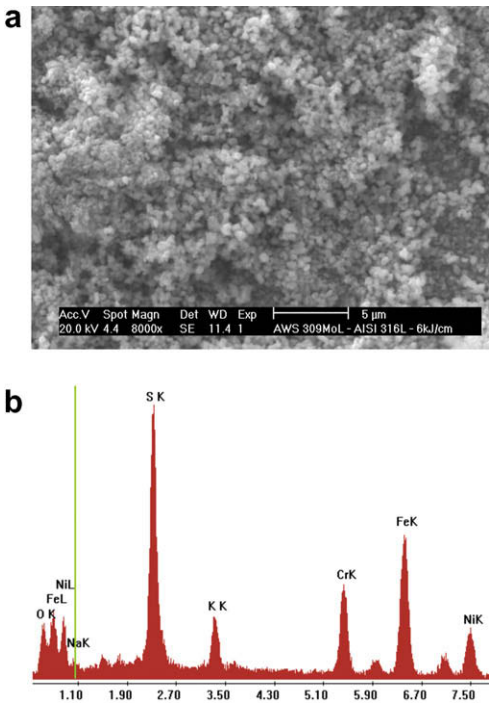

Fig. 9. (a) Morphology of iron sulfide fine film and (b) EDX analysis of corrosion products.

sulfur and iron, thus characterizing iron sulfide as the product of corrosion. Further evaluation in a region more distant from the weld bead, showed the precipitation of considerable quantity of particles on the surface. The aspect of this region is shown in Fig. 8a. Cavities whose aspect is similar to that shown in Fig. 6a, in which the contours of the austenite grain can be noticed (Fig. 8b), were also present in this region.

Iron sulfide fine film morphology is shown in Fig. 9a. It is observed that the layer is formed by countless very fine agglomerated particles. The EDX analysis (Fig. 9b) of the layer presents high contents of iron and sulfur besides chromium, indicating to be an iron sulfide layer. The presence of oxygen was not observed, reinforcing the idea that in the 300 °C temperature the corrosive substances are associated to sulfurated compounds.

As observed in the superficial characterization, in 300 °C temperature, the corrosion product formed was only iron sulfide. The presence of this type of corrosion product indicates that the attack is mainly due to the action of corrosive substances originating from sulfurated compounds. According to the the literature, the main corrosion types that act in this temperature range are high temperature hydrogen sulfide corrosion (HTHC) and naphthenic acid corrosion.

HTHC happens due to the presence of H_2S in high temperature conditions, above 260 °C, and it is characteristic of petroleum refinery equipments as distillation towers that process petroleum with high sulfur contents [5]. In general, this type of corrosion among the iron contained in the steel and H_2S, results in the following reaction:

$$Fe + H_2S \rightarrow FeS + H_2 \quad (4)$$

The surface of the equipment that suffers from HTHC is covered with a layer of iron sulfide a corrosion product, which is a black and slightly adherent material. The stoichiometric iron sulfide compounds found as corrosion products related to sulfur-rich medium and higher temperature are troilite (FeS), pyrite and macassite (Fe_2S) [3]. Silva et al. [6] evaluated the corrosion type

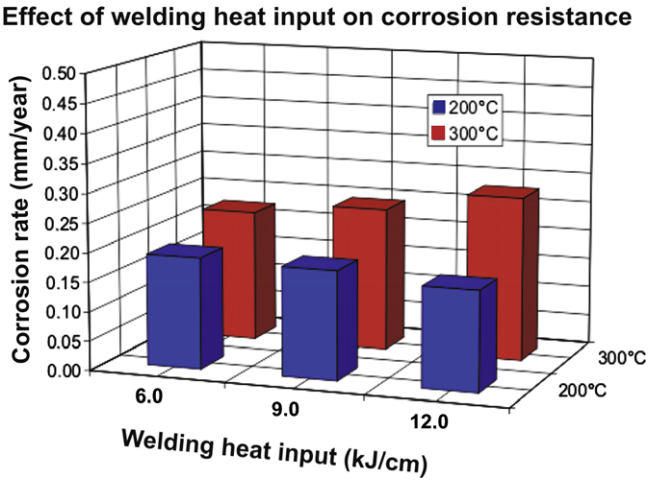

Fig. 10. Variation of the HAZ corrosion rate with welding heat input.

caused by a heavy petroleum that contained 4% of sulfur, and concluded that the corrosive process was caused for sulfurated compound, mainly H_2S, indicating treats of a HTHC process.

The naphthenic acid corrosion (NAC) has been a problem in the refining industry. Several researches have studied the factors that affect naphthenic acid corrosion, and have also studied some critical points such as the presence of naphthenic acid that confers to oil a high corrosiveness [1,25–28]. One of the methods to measure the corrosiveness of crude oils is the TAN "Total acid number". Petroleum TAN greater than 0.5 generally contains enough naphthenic acids to promote corrosion. Other critical points that affect the NAC are the processing temperature of the equipment. The NAC occurs in cruds distillation units in the 220–400 °C temperature range [1,8,29,30]. In general, the reactions involved in the NAC are described typically by

$$Fe + 2RCOOH \rightarrow Fe(RCOO)_2 + H_2 \quad (5)$$

$$Fe + H_2S \rightarrow FeS + H_2 \quad (6)$$

$$Fe(RCOO)_2 + H_2S \rightarrow FeS + 2RCOOH \quad (7)$$

It can be noticed in Eq. (5) that strong iron naphthenates are soluble in oil and the surface is free from film of corrosion products. Nevertheless, in the presence of H_2S an iron sulfide film can be formed on the surface, offering, in some cases, a little protection to the steel surface (Eqs. (6) and (7)).

Although the TAN of the crude oil used in this work cannot be revealed due to contract reasons, it can be said that its contents is enough to promote the NAC, together with the range of temperatures employed in this work and the presence of iron sulfide film. These factors pointed the NAC as the main corrosion process responsible for the attack of 316L steel at 300 °C temperature.

3.3. Corrosion rate evaluation

The rate of corrosion in the HAZ of the 316L austenitic stainless steel is shown in Fig. 10. It can be observed that there is no significant variation on the corrosion rate among the welding heat inputs used for treatment at 200 °C. This result is coherent with the observation of the surface, in which no significant changes in the aspect of the superficial corrosion were noticed, among the test objects, for the three welding conditions used. The smallest corrosion rate presented by the material treated at 200 °C can be attributed to the CO_2 corrosion, once the carbonic acid (H_2CO_3) presents smaller corrosive effect when compared with naphthenic acids and H_2S.

Nevertheless, at 300 °C, the variation in the rate of corrosion was more significant, following a tendency of growth with the increase of the welding heat input. This tendency of increase in the rate of corrosion was also noticed through the superficial characterization, in which the intensity of the corrosive attack on the surface increases with the increase of the welding heat input. The largest corrosive attack presented by samples treated at 300 °C temperature was attributed to the temperature increase that provides the action of highly corrosive substances such as naphthenic acid and H_2S. The variation of the corrosion rate as a function of the welding heat input was attributed to the increase of the heat input that leads to reduction in the cooling rate, causing a drastic increase in the precipitation rate of chromium carbides, as well as in the HAZ extension.

4. Conclusions

Based on the experimental results obtained for the welding conditions and thermal treatment in petroleum used in this work, it was possible to conclude that the thermal cycle of weld, regardless of the energy applied, was enough to cause alteration in the heat affected zone (HAZ) of the AISI 316L austenitic stainless steel, making this region more likely to suffer from corrosion. For temperatures of 200 °C there was formation of both iron oxide and iron sulfide as products of corrosion. At 300 °C, however, the product of corrosion was basically iron sulfide. Two types of corrosion were observed for heat treatment at 200 °C temperature the, one caused by the combination of carbonic acid and H_2S; however, the CO_2 corrosion was the predominant type with H_2S corrosion in smaller scale. For samples heat treated in petroleum immersion at 300 °C temperature, evidences of naphthenic acid corrosion or a combination of naphthenic acid corrosion and high temperature hydrogen sulfide corrosion with high corrosiveness were observed. The variation in the welding heat input causes a variation in the value of the rate of corrosion at 300 °C.

Acknowledgements

The authors are grateful to ENGESOLDA, LACAM and LCL laboratories. They are also grateful to PETROBRAS for its collaboration and to Brazilian research agencies (CNPq, FINEP e ANP/PRH-31) for financial support.

References

[1] Babaian-Kibala E, Craig Jr HL, Rusk GL, Blanchard KV, Rose TJ, Uehlein BL. Naphthenic acid corrosion in a refinery setting. Corrosion 93 (paper 631). New Orleans: NACE International; 1993.
[2] Medvedeva ML. Specifics of high-temperature corrosion processes during oil recovery. Chem Petrol Eng 2000;36:749–54.
[3] Tebbal S. Critical review of naphthenic acid corrosion. Corrosion 99 (paper 380). Dallas, Texas: NACE International; 1999.
[4] Nugent MJ, Dobis JD. Experience with naphthenic acid corrosion in low tan crudes. Corrosion 98 (paper 577). San Diego, CA: NACE International; 1998.
[5] Chernov VY. Influence of oxygen and hydrogen sulfide on the carbonic acid corrosion of welded metal structure of oil and gas equipment. Mater Sci 2001;37:808–15.
[6] Silva CC, Machado JPSE, Sobral-Santiago AVC, de Sant'Ana HB, Farias JP. High-temperature hydrogen sulfide corrosion on the heat affected zone of the AISI 444 stainless steel caused by Venezuelan heavy petroleum. J Petrol Sci Eng 2007;59(3–4):219–25.
[7] Cosultchi A, Garciafigueroa E, Garcia-Borquez A, Reguera E, Yee-Madeira H. Petroleum solid adherence on tubing surface. Fuel 2001;80:1963–8.
[8] Turnbull A, Griffiths A. Corrosion and cracking of weldable 13 wt% Cr martensitic stainless steel for application in the oil and gas industry. Corros Eng, Sci Technol 2003;38(1):21–49.
[9] Folkhard E. Welding metallurgy of stainless steels. New York: Springer-Verlag; 1988.
[10] Farraro T, Stellina Jr RM. Materials construction for refinery applications. Corrosion 96 (paper 614). Denver, Colorado: NACE International; 1996.
[11] Kou S. Welding metallurgy. New York: John Wiley & Sons; 2003.
[12] Weiss B, Stickler R. Phase instabilities at high temperature exposure of 316 austenitic stainless steel. Metall Trans A 1972;3:851–64.
[13] Silva CC, Almeida Neto JC, de Sant'Ana HB, Farias JP. Microstructural changes in the AISI 410S stainless steel HAZ – effects on corrosion resistance. Soldagem Inspeção 2006;11:188–99 [in Portuguese].
[14] ASTM standards. Standard G 1–90, 1–8. Philadelphia, PA: ASTM; 1993.
[15] Cui Y, Lundin CD. Austenite-preferential corrosion attack in 316 austenitic stainless steel weld metals. Mater Des 2007;28:324–8.
[16] Matula M, Hyspecka L, Svoboda M, Vodarek V, Dagbert C, Galland J, et al. Intergranular corrosion of AISI 316L steel. Mater Charact 2001;46(2–3):203–10.
[17] Shaikh H, Rao BPC, Gupta S, George RP, Venugopal S, Sasi B, et al. Assessment of intergranular corrosion in AISI Type 316L stainless steel weldments. Brit Corros J 2002;37(2):129–40.
[18] Devine TM. The mechanism of sensitization of austenitic stainless steel. Corros Sci 1990;30(2–3):135–51.
[19] Beneke R, Sandenbergh RF. The influence of nitrogen and molybdenum on the sensitization properties of low-carbon austenitic stainless steels. Corros Sci 1989;29(5):543–55.
[20] Luz TS, Farias JP, Lima Neto P. Use of double loop electrochemical potentiokinetic reaction (DL-EPR) to evaluate the sensitization of austenitic stainless steels after welding. Weld Int 2006;20:959–64.
[21] Majidi AP, Streicher MA. Four nondestructive eletrochemical tests for detecting sensitization in type 304 and 304L stainless steels. Nucl Technol 1986;75:584–93.
[22] ASTM book of standards. Standard A262-93a, 42–57. Philadelphia, PA: ASTM; 1993.
[23] Silva CC, Ramos Jr JMB, Almeida Neto JC, Sant'Ana HB, Farias JP. Corrosion resistance evaluation of the stainless steels used as petroleum distillation column coating. Petro Quim 2006;XXX:106–12.
[24] Machado JPSE, Silva CC, Sobral-Santiago AVC, de Sant'Ana HB, Farias JP. Effect of temperature on the level of corrosion caused by heavy petroleum on AISI 304 and AISI 444 stainless steel. Mater Res 2006;9(2):137–42.
[25] Slavcheva E, Shone B, Turnbull A. Factors controlling naphthenic acid. Corrosion 98 (paper 579). San Diego, CA: NACE International; 1998.
[26] Tebbal S, Kane RD. Assessment of crude oil corrosivity. Corrosion 98 (paper 578). San Diego, CA: NACE International; 1998.
[27] Slavcheva E, Shone B, Turnbull A. Review of naphthenic acid corrosion in oil refining. Brit Corros J 1999;34(2):125–31.
[28] Babaian-Kibala E, Nugent MJ. Naphthenic acid corrosion literature survey. Corrosion 99 (paper 378). Dallas, Texas: NACE International; 1999.
[29] Hopkinson BE, Peñuela LE. Naphthenic acid corrosion by Venezuelan crudes. Corrosion 97 (paper 502). New Orleans, LA: NACE International; 1997.
[30] Kane RD, Cayard MS. A comprehensive study on naphthenic acid corrosion. Corrosion 2002 (paper 2555). Denver, CO: NACE International; 2002.